EUROPEAN ORGANIZATION FOR NUCLEAR RESEARCH

NEUTRON-PROTON CHARGE EXCHANGE SCATTERING FROM 9 TO 23 GeV/c *)

V. Böhmer, J. Engler, W. Flauger, B. Gibbard, R. Hartung,
F. Mönnig, K. Pack, K. Runge and H. Schopper

Institut für Experimentelle Kernphysik, Karlsruhe, Germany

and

CERN, Geneva, Switzerland

ABSTRACT

The differential cross-sections for neutron-proton charge exchange scattering have been measured with high statistics in the region of momentum transfer squared $0.002 < |t| \leq 0.400$ (GeV/c)^2 and for incident neutron momenta $9 < p \leq 23$ GeV/c.

Geneva - 19 March 1976

(Submitted to Nuclear Physics)

*) Work supported in part by the Bundesministerium für Forschung und Technologie, Bonn, Germany.

1. INTRODUCTION

In preparing an np charge exchange scattering experiment for the Serpukhov accelerator[1], measurements of this reaction were performed at the CERN Proton Synchrotron (PS). The aim was to obtain high statistics data and to achieve a good normalization. At the same time an experimental technique was to be developed which could cope with the lower cross-sections and higher background at Serpukhov energies. The technique was therefore essentially the same as that described in Ref. 1 with some minor differences which are discussed in the following.

2. EXPERIMENTAL TECHNIQUE

The experimental arrangement used is shown in Fig. 1. A neutron beam with a broad momentum distribution was taken off an internal Be target at $0°$. Its shape was 1×2 cm^2 at the position of the external liquid-hydrogen target. The photons in the beam were filtered out with an absorber of lead to a fraction of less than 1%, and the contamination of K^0 and $\bar{n}$ could, according to the thermodynamical model[2], be neglected.

The neutron flux was determined with two monitor telescopes in the beam, each consisting of an anticounter, a converter (about 1 cm of carbon and iron, respectively), and two trigger counters in coincidence. During low-intensity runs the efficiency of both monitors (2.5% and 7.0%) were calibrated against a sampling total absorption counter (STAC)[3], whose efficiency was measured to be (100 ± 1)%. The two monitors were stable in relation to each other within 5%. The beam contained typically 2.3×10^6 neutrons per burst.

The spectrum of the beam as function of the neutron momentum p was measured with the STAC. As the spectral shape crucially affects the normalization and the energy dependence of the cross-sections, the spectrum was carefully measured using several trigger counters inserted into the STAC. The response of the STAC as a function of energy was determined with protons, and a correction of about 3% in the energy scale was applied in order to take into account the charge difference between an incoming proton and neutron. Also, rate effects were studied. The final spectrum, which was taken at 50 kHz counting rate, is shown in Fig. 2. The errors indicated are mainly due to the uncertainties in the energy calibration and resolution as determined with protons. At very low momenta, the resolution of STAC is rather poor ($\Delta p/p \simeq 1$). Therefore below 3 GeV/c the spectrum was extrapolated from the higher momentum part.

The target was constructed as a Čerenkov counter in order to have an additional kinematic constraint, allowing separation of elastic events from the background. From the amount of light output, the path length of the proton -- and thereby the interaction point within the target -- could be determined[4]. For a throughgoing particle the spatial resolution was $\sigma = \pm 3$ cm, a figure similar to that reported in Ref. 4. The recoil neutron angle could therefore be determined to $\pm 4°$.

The beam passed the target close to the edge so as to minimize the scattering of the low-energy recoiling neutrons in the hydrogen, which destroys the coplanarity of an elastic event.

The forward proton was detected in a spark chamber magnetic spectrometer. A 2 m magnet bent the protons away from the beam. A particle in the spectrometer was signalled by a coincidence of three trigger counters (P1,P2,P3) and, in order to suppress background events, by a veto in P1 for a signal exceeding an upper threshold corresponding to about three throughgoing particles.

The thresholds of the neutron counters were set at 0.10 MeV electron energy using the Compton electrons from a ^{60}Co source, ensuring an onset of the detection efficiency for neutrons at about 0.8 MeV. The efficiency was calculated with the Oak Ridge Monte Carlo program 05S, as described in detail in Ref. 1.

3. DATA ANALYSIS

The data analysis followed closely the line described in Ref. 1. The proton track was reconstructed, requiring at least three chambers out of four to be set in the top and side views both before and behind the magnet. Under the actual background conditions of the experiment, the chamber efficiencies were measured to be 0.95 ± 0.02; thus a track was found in each of the four views with a probability of 98.6% and the whole trajectory with 94.5% probability.

In the neutron counter a signal on both sides of the scintillator was required. The point of interaction could be determined by the difference in time of arrival of the light at the two ends. This position was taken into account when calculating the time of flight. A cut corresponding to the energy of the elastic recoil neutron as determined from the proton arm was applied to the pulse height in the neutron counter. Events with too high a pulse height were rejected.

A kinematic fit was accomplished as described in Ref. 1, then the elastic events were determined from the coplanarity. As an example, the distribution of the difference of the azimuthal angles is shown in Fig. 3 for a low and a high momentum transfer. For small $|t|$ the distribution is broader since the proton azimuthal angle is less well determined for the very small scattering angles owing to the finite resolution of the wire chambers ($\sigma = 0.4$ mm). In the whole kinematic region the elastic signal could well be separated from the background. The fraction to be subtracted from under the elastic peak was typically 10% and almost independent of the t- and p-region.

It turned out that the information coming from the Čerenkov light in the target was not necessary for separating the elastic events from the background. Therefore this constraint was not used in the final analysis in order to avoid systematic errors in additional efficiency measurements.

In total, about 12×10^4 events were recognized as elastic.

4. ABSOLUTE NORMALIZATION AND CORRECTIONS

The total neutron flux was determined from the monitor placed farthest downstream; its efficiency was measured to be (7.0 ± 0.7)%. The flux per momentum bin was then calculated using the spectrum as given in Fig. 2. The indicated extrapolation to zero momentum gives rise to an additional uncertainty in the normalization of about 1%.

The acceptance of the apparatus was calculated with a Monte Carlo program which was also used for the set-up of Ref. 1.

Finally, the following corrections had to be applied to the cross-sections as calculated from the observed elastic events:

i) The high counting rates in the anticounter system vetoed good events. These dead-time losses were measured electronically and amounted to 5%.

ii) The high counting rates in the neutron counters implied that for some of the elastic events an additional counter fired accidentally. This effect was studied electronically by chance coincidences, and in an off-line analysis by looking at events with two neutron counters set. The elastic events found in these data amounted to about 5%, whereas from the rates an effect of about 3% was deduced.

iii) The upper threshold in the trigger counter P1 which vetoed high pulse heights, caused losses in the elastic event rate owing to the Landau tail, giving rise to a correction of 20%. This figure was measured with a proton beam traversing the spectrometer.

iv) A correction of 5% was made to compensate for absorption loss of the neutron beam in the hydrogen target and the material between the target and the second monitor.

All the corrections applied to the cross-sections and the corresponding uncertainties are listed in Table 1. Also listed are the uncertainties in the flux determination of the beam and in the way the background was subtracted under the elastic peak. All these errors result in a total uncertainty of 12.5% in the absolute cross-sections.

5. RESULTS

The differential cross-sections are given in Table 2 together with the statistical errors. The extreme right-hand column contains the errors due to the neutron detection efficiency calculation. They affect only the t-distribution but not the p-dependence of the cross-sections. In the bottom line the uncertainty of the incident momentum spectrum is given, which is relevant for the p- but not for the t-dependence. In addition, there is the 12.5% normalization error as explained above.

Figure 4 shows how the t-distribution for 19-21 GeV/c primary momentum compares with existing results by Engler et al.[5] and Kreisler et al.[6]. The different data show almost the same t-dependence. The high-statistics data of this experiment demonstrate that there is no structure around $|t| \approx 0.1$ $(GeV/c)^2$ in the momentum region covered by this experiment, as might have been suspected from the previous data.

In Fig. 5 the extrapolated cross-sections at t = 0 are shown for the six p-intervals, together with corresponding figures by Miller et al.[7] and of other experiments. The extrapolation was done as outlined in Ref. 1. The values of this experiment agree rather well with those of Ref. 3 and confirm the momentum dependence. Fitting the cross-sections at t = 0 to a fall-off like p^{-n}, an exponent of $n = 1.92 \pm 0.09$ is obtained when taking the data of this experiment and the data of Refs. 2, 5, 6, and 7 in the momentum region $5 \leq p \leq 25$ GeV/c.

Acknowledgements

We would like to thank Mrs. I. Klanner as well as Messrs. H. Keim, K. Ratz and C. Weber for their work in carrying out the experiment. The excellent work of the Hydrogen Target Group under the direction of Mr. L. Mazzone is gratefully acknowledged. We are indebted to the EP Technical Assistance Group under Mr. G. Muratori for the design of a collimator, and to the PS running staff for their skilful operation of the accelerator.

REFERENCES

1) The experiment and its results are described in the preceding article.

2) J. Ranft and J.T. Routti, CERN Lab. II-RA/71-4 (1971).

3) J. Engler, W. Flauger, B. Gibbard, F. Mönnig, K. Runge and H. Schopper, Nuclear Instrum. Methods 106 (1973) 189.

4) F. Sergiampietri *in* Proc. 1973 Internat. Conf. on Instrumentation for High-Energy Physics, Frascati (CNEN, Frascati, 1973), p. 430.

5) J. Engler, K. Horn, F. Mönnig, P. Schludecker, W. Schmidt-Parzefall, H. Schopper, P. Sievers, H. Ullrich, R. Hartung, K. Runge and Yu. Galaktionov, Phys. Letters 34B (1971) 528.

6) M.N. Kreisler, M.B. Davis, M.J. Longo and D.D. O'Brien, Nuclear Phys. B84 (1975) 3.

7) E.L. Miller, M. Elfield, N.W. Reay, N.R. Stanton, M.A. Abolins, M.T. Lin and K.W. Edwards, Phys. Rev. Letters 26 (1971) 984.

Table 1

Correction factors and uncertainties

Correction	Correction factor	Uncertainty (%)
Track-finding efficiency	1.06	±5
Dead-time of antisystem	1.05	±2
Neutron counter rate effects	1.04	±2
Trigger counter upper threshold	1.20	±3
Beam loss upstream of Monitor 2	0.95	±1
Monitor efficiency	1.0	±10
Spectrum extrapolation to zero	1.0	±1
Beam contamination (γ and K^0)	1.0	±2
Background subtraction	1.0	±3
Total	1.32	±12.5

Table 2

Differential cross-sections for neutron-proton charge exchange for momentum intervals (in GeV/c). The indicated uncertainties are statistical errors only. The extreme right-hand column and the bottom line show possible systematic t-dependent and p-dependent errors, respectively. The additional absolute normalization uncertainty is ±12.5%.

$\|t\|$ interval $(GeV/c)^2$	$d\sigma/dt$ $[\mu b/(GeV/c)^2]$						%
	9-12	12-15	15-17	17-19	19-21	21-23	
0.002-0.003	617 ± 35	368 ± 25	318 ± 24	264 ± 17	245 ± 15	198 ± 15	9
0.003-0.004	605 ± 31	354 ± 20	302 ± 18	250 ± 13	216 ± 11	186 ± 12	6
0.004-0.005	584 ± 29	379 ± 19	264 ± 16	256 ± 13	197 ± 10	166 ± 11	11
0.005-0.007	539 ± 20	370 ± 14	252 ± 12	232 ± 10	187 ± 8	159 ± 8	11
0.007-0.009	530 ± 21	339 ± 14	223 ± 12	204 ± 9	165 ± 8	160 ± 9	10
0.009-0.012	505 ± 19	308 ± 12	255 ± 11	191 ± 8	161 ± 7	138 ± 7	7.5
0.012-0.016	437 ± 16	309 ± 11	220 ± 10	181 ± 8	154 ± 6	112 ± 6	6.5
0.016-0.020	419 ± 16	267 ± 11	204 ± 10	174 ± 7	137 ± 6	119 ± 6	6.5
0.020-0.024	378 ± 16	249 ± 11	183 ± 10	148 ± 7	129 ± 6	103 ± 6	5.5
0.024-0.028	331 ± 15	202 ± 10	151 ± 9	127 ± 7	116 ± 6	92 ± 6	5.0
0.028-0.034	302 ± 14	190 ± 8	150 ± 8	120 ± 6	104 ± 5	82 ± 5	4.0
0.034-0.042	307 ± 12	182 ± 8	131 ± 7	117 ± 6	91 ± 5	84 ± 4	3.5
0.042-0.050	283 ± 12	164 ± 8	110 ± 7	106 ± 6	86 ± 4	68 ± 4	3.5
0.050-0.060	261 ± 11	158 ± 7	107 ± 6	89 ± 5	81 ± 4	65 ± 4	2.5
0.060-0.070	247 ± 10	147 ± 7	105 ± 6	80 ± 5	74 ± 4	59 ± 4	1.5
0.070-0.090	216 ± 8	132 ± 6	93 ± 5	73 ± 4	67 ± 3	58 ± 3	-
0.090-0.120	187 ± 7	114 ± 5	87 ± 5	66 ± 4	57 ± 3	52 ± 3	-
0.120-0.160	121 ± 6	100 ± 5	73 ± 4	64 ± 3	53 ± 2	49 ± 3	-
0.160-0.200	118 ± 8	82 ± 5	62 ± 4	53 ± 3	48 ± 2	40.5 ± 2	-
0.200-0.250	-	58 ± 4	44 ± 3	37 ± 2	35 ± 2	30.5 ± 2	-
0.250-0.300	-	51 ± 4	36 ± 3	33.5 ± 3	25.5 ± 2	23.5 ± 2	-
0.300-0.400	-	-	21.5 ± 2	18.5 ± 2	15 ± 2	14.5 ± 2	-
%	12	9	7	5	5	7	

Figure captions

Fig. 1 : The experimental layout. At the bottom the arrangement of the neutron counters is shown as seen when looking in the beam direction.

Fig. 2 : The spectrum of the incident neutrons as measured with a total absorption counter.

Fig. 3 : The difference $\Delta\phi$ in the azimuthal angle of the forward proton and the recoiling neutron for small and large $|t|$-intervals.

Fig. 4 : $np \to pn$ differential cross-sections for neutron momenta between 18 and 21 GeV/c.

Fig. 5 : The differential cross-sections extrapolated to $t = 0$ as function of the neutron momentum. (For the extrapolation, see Ref. 1.)

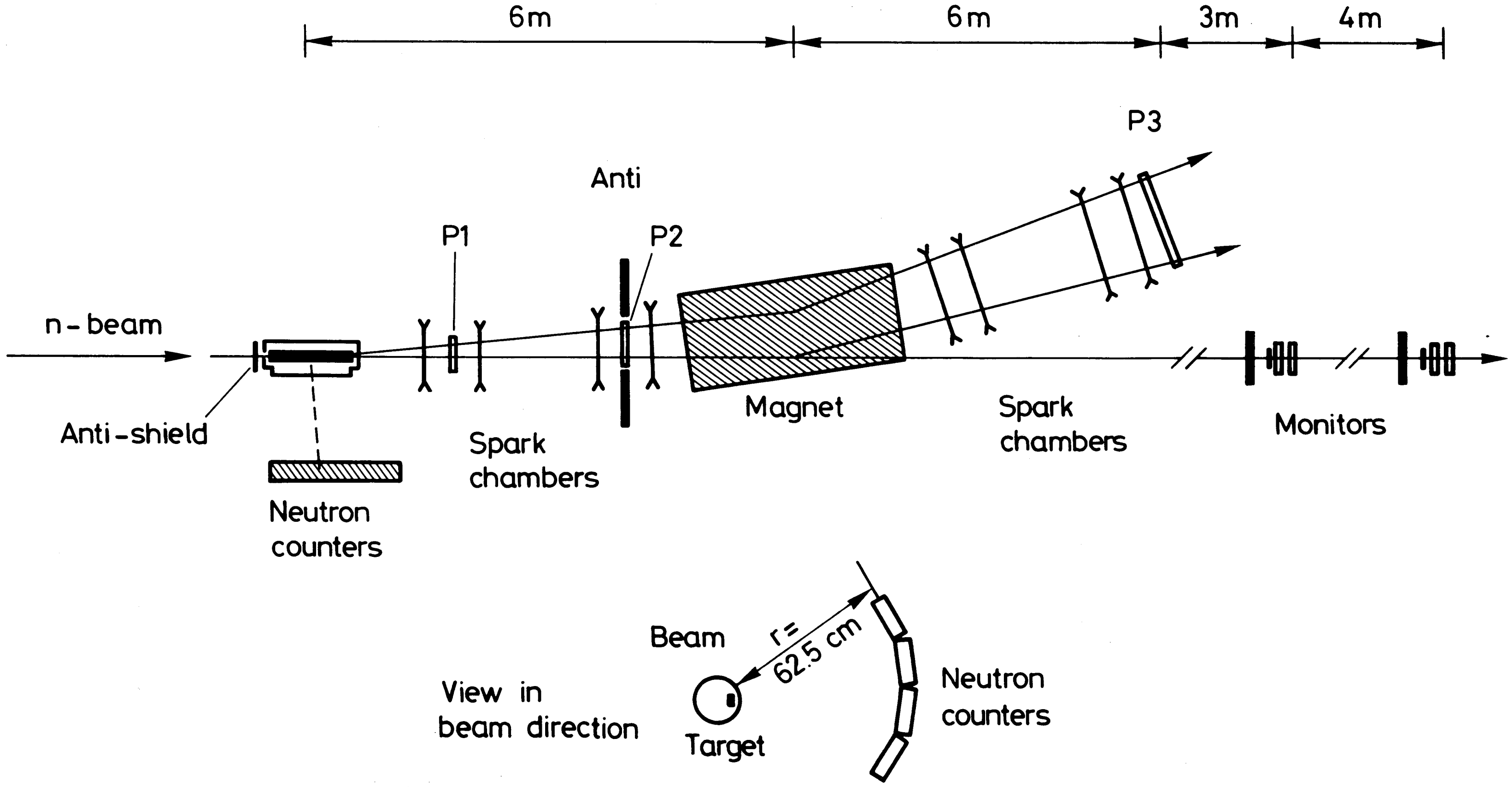
6m
6m
3m
4m
P3
Anti
P1
P2
n-beam
Anti-shield
Magnet
Spark
chambers
Spark
chambers
Monitors
Neutron
counters
Beam
r=
62.5 cm
View in
beam direction
Target
Neutron
counters

Fig. 1

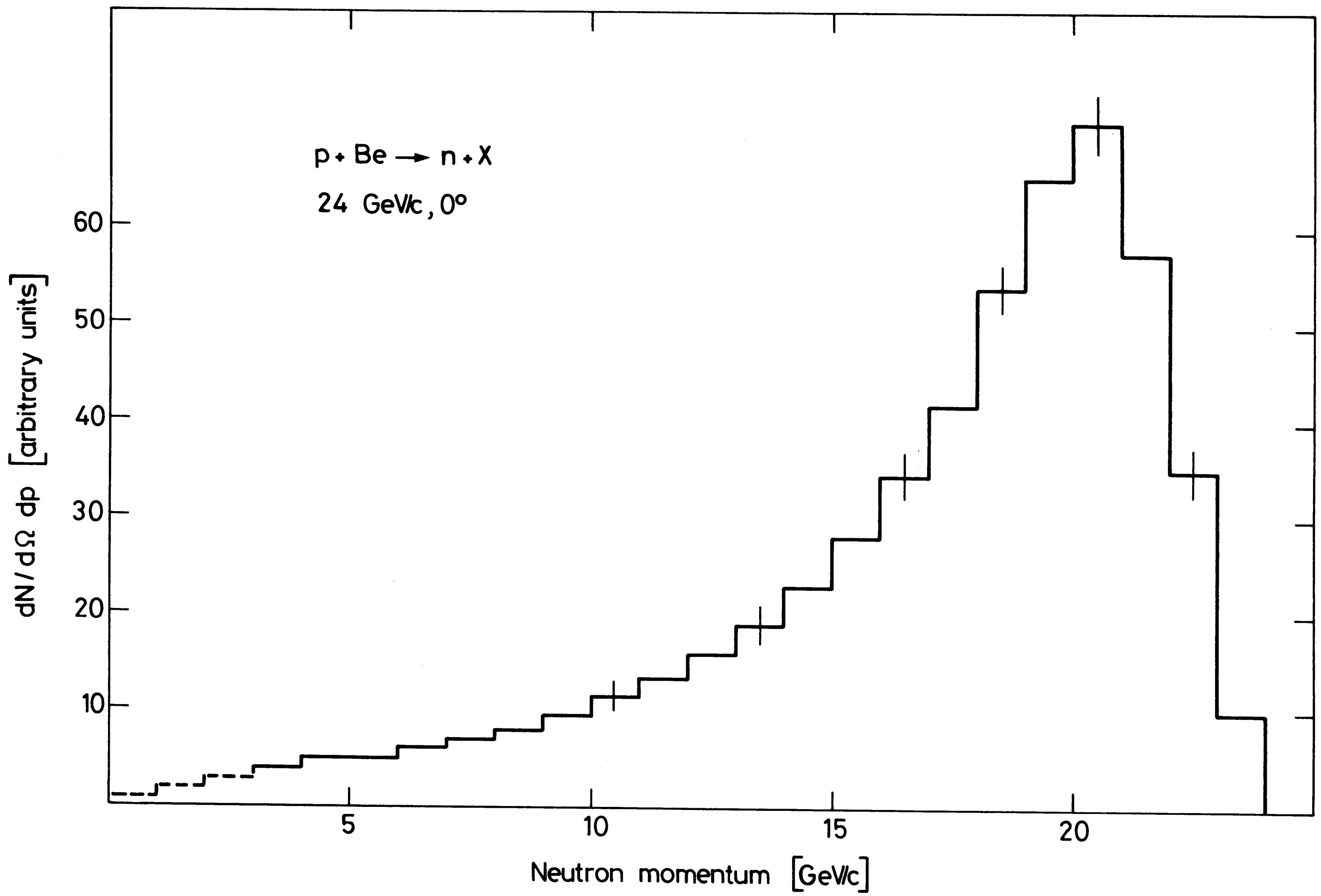
p + Be → n + X
24 GeV/c, 0°
dN/dΩ dp [arbitrary units]
60
50
40
30
20
10
5
10
15
20
Neutron momentum [GeV/c]

Fig. 2

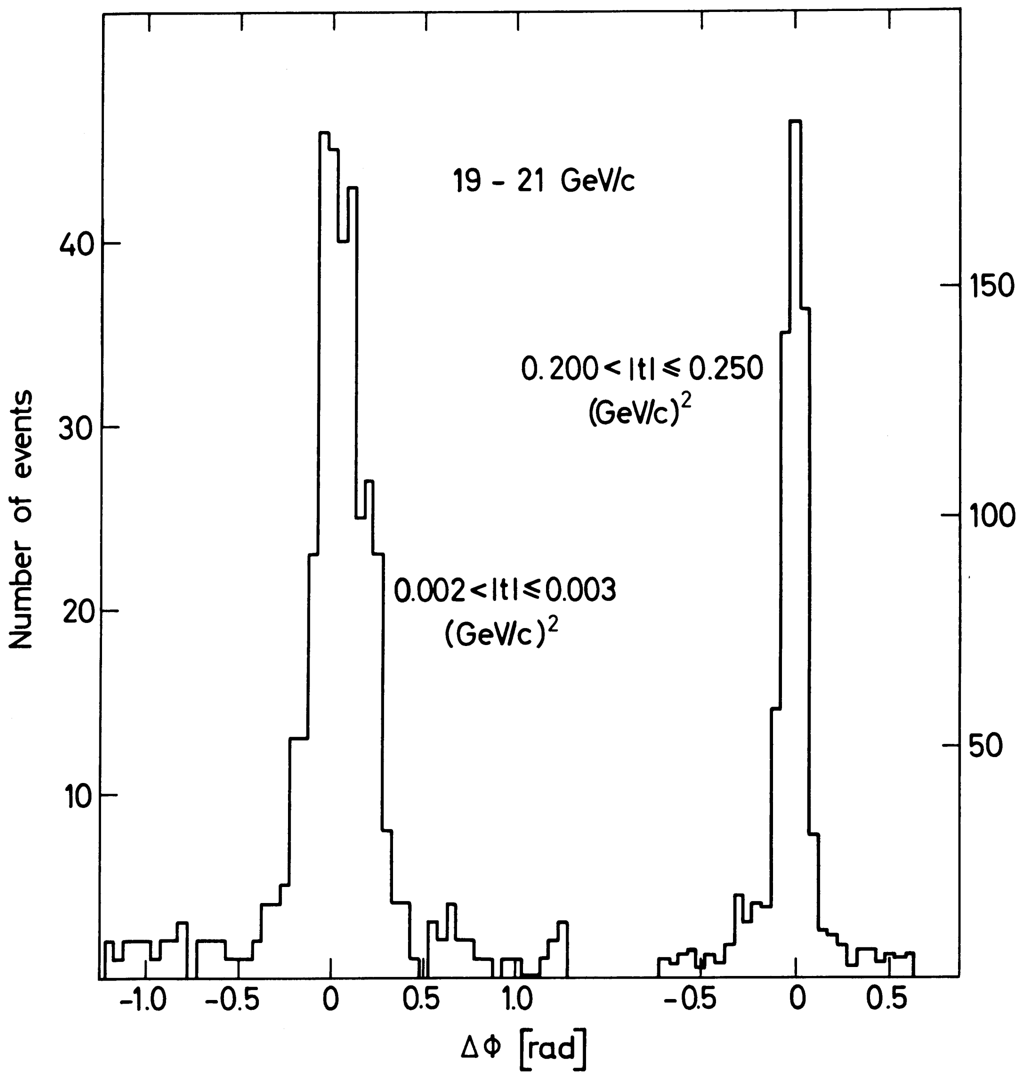
19 - 21 GeV/c
0.200 < |t| ≤ 0.250 (GeV/c)^2
0.002 < |t| ≤ 0.003 (GeV/c)^2
Number of events
40
30
20
10
150
100
50
-1.0
-0.5
0
0.5
1.0
-0.5
0
0.5
ΔΦ [rad]

Fig. 3

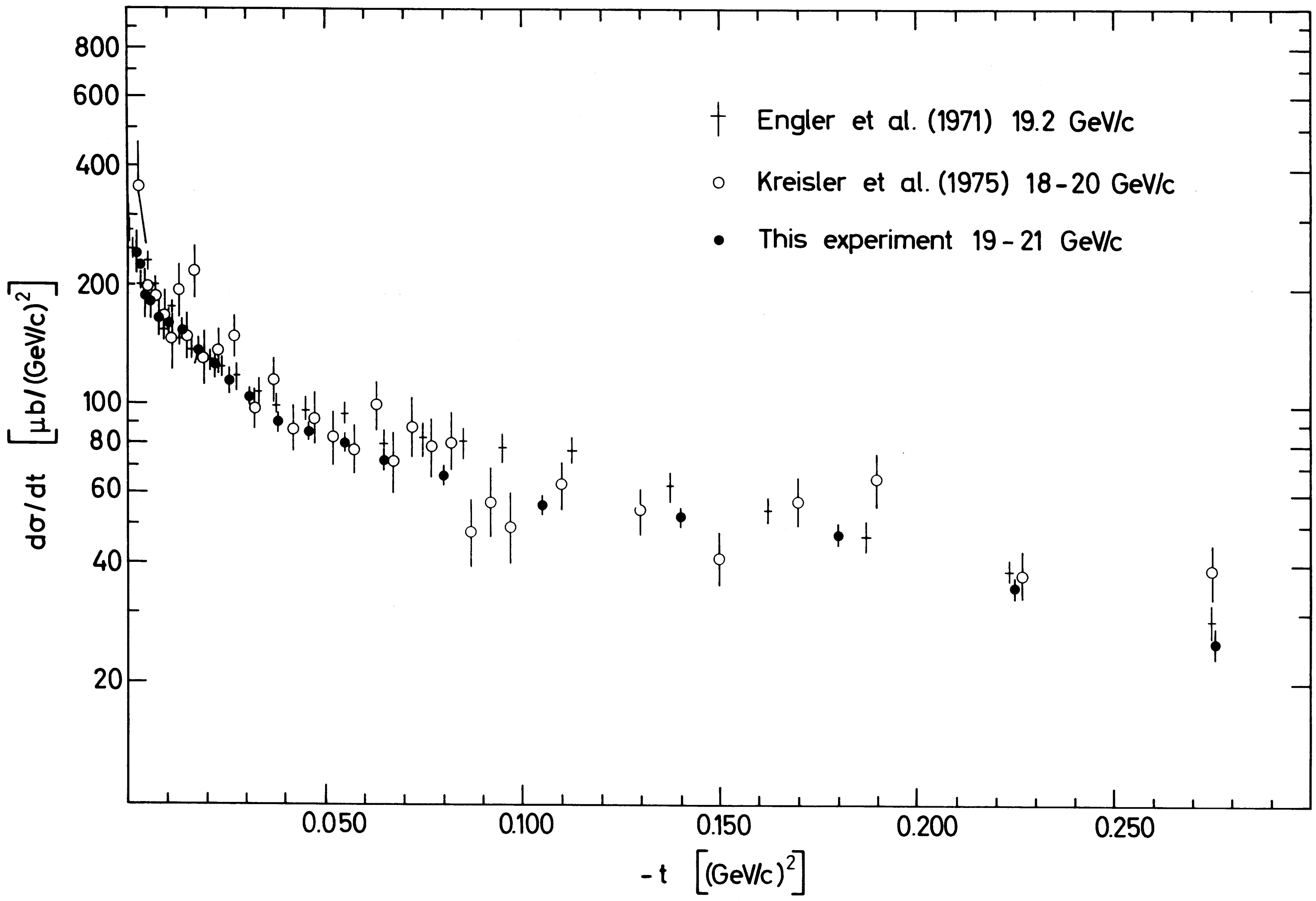

Engler et al. (1971) 19.2 GeV/c
Kreisler et al. (1975) 18-20 GeV/c
This experiment 19-21 GeV/c
dσ/dt [μb/(GeV/c)^2]
800
600
400
200
100
80
60
40
20
0.050
0.100
0.150
0.200
0.250
-t [(GeV/c)^2]

Fig. 4

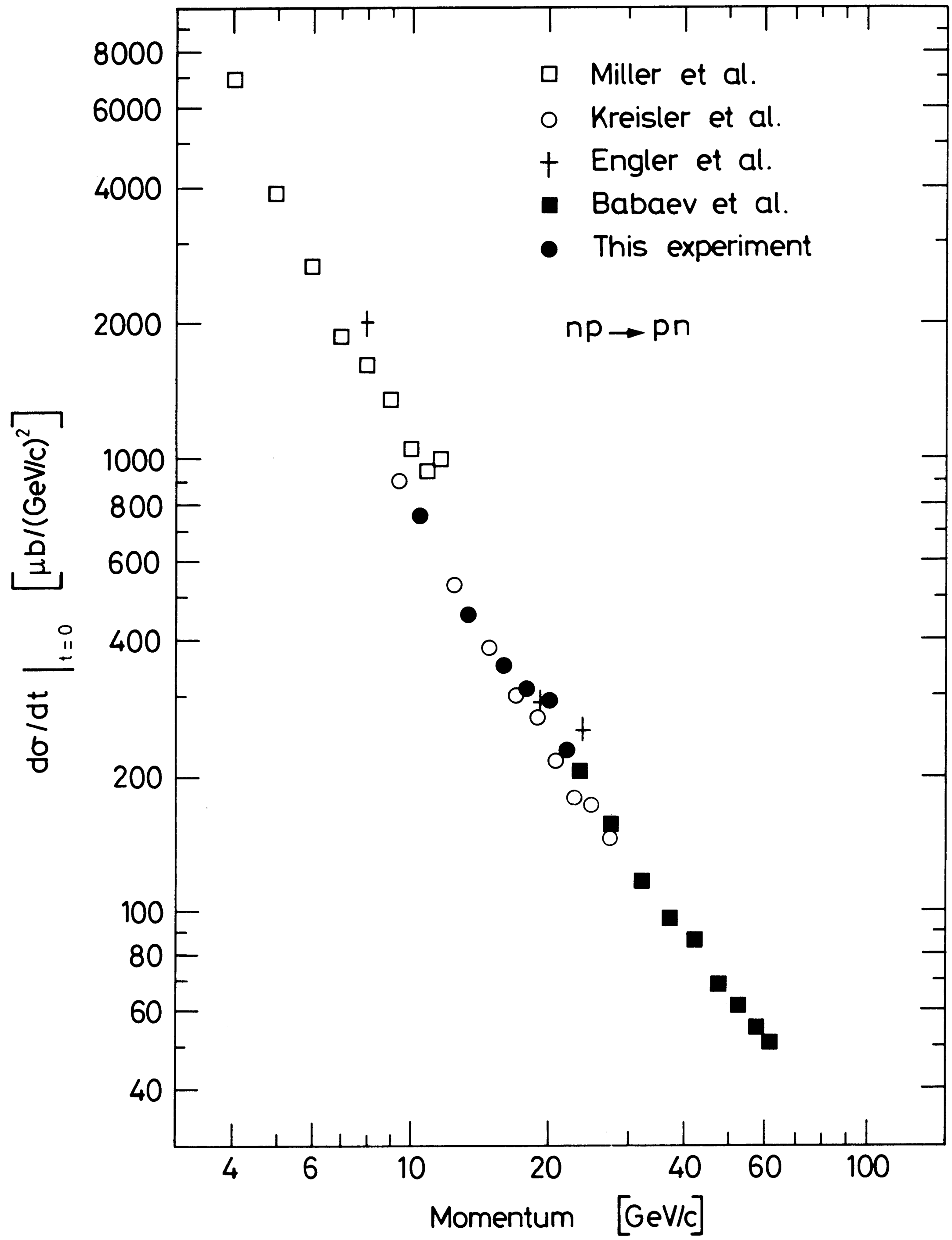

8000
6000
4000
2000
1000
800
600
400
200
100
80
60
40
4
6
10
20
40
60
100
Miller et al.
Kreisler et al.
Engler et al.
Babaev et al.
This experiment
np → pn
dσ/dt |t=0 [μb/(GeV/c)²]
Momentum [GeV/c]

Fig. 5